Insulator-to-metal transition in polythiophene

F. C. Lavarda,* M. C. dos Santos, D. S. Galvão, and B. Laks
Instituto de Física "Gleb Wataghin," Universidade Estadual de Campinas, 13081 Campinas, São Paulo, Brazil
(Received 9 July 1993)

In the present work, the electronic structure of polythiophene at several doping levels is investigated by the use of the Hückel Hamiltonian with σ-bond compressibility. Excess charges are assumed to be stored in conformational defects of the bipolaron type. The Hamiltonian matrix elements representative of a bipolaron are obtained from a previous thiophene oligomer calculation, and then transferred to very long chains. Negative factor counting and inverse iteration techniques have been used to evaluate densities of states and wave functions, respectively. Several types of defect distributions were analyzed. Our results are consistent with the following: (i) the bipolaron lattice does not present a finite density of states at the Fermi energy at any doping level; (ii) bipolaron clusters show an insulator-to-metal transition at 8 mol % doping level; (iii) segregation disorder shows an insulator-to-metal transition for doping levels in the range 20–30 mol %.

I. INTRODUCTION

In spite of an enormous amount of theoretical and experimental work on conducting polymers in the last decade,[1] some fundamental aspects of their electronic behavior remain unsolved. In particular, the mechanisms involved in the transition to a metallic regime is an open and polemical question.

It is more or less accepted that solitons and/or polarons are the major charge carriers involved in the conduction processes of polyacetylene (PA),[2] the structurally simplest conducting polymer. PA has a degenerate ground state while polyheterocyclies like polypyrrole and polythiophene (PT), polyaniline, and others have a nondegenerate ground state related to the nonenergetic equivalence of their two limiting mesomeric forms. These are the aromatic and quinoid structures, with the quinoidal form having higher energy. In these polymers, the addition or removal of charge induces local chain distortions with the appearance of intragap states associated with polarons and bipolarons. It is assumed that adjacent polarons are unstable and lead to the formation of bipolarons, but the details involved in the process are not well understood. PT is of special interest among conducting polymers because it can be prepared in soluble form, is chemically stable, and easily processible. Compounds based on thiophene present interesting properties as electrochromism and thermochromism.

Distinct transport properties are observed in polymers at different doping levels. The appearance of metallic behavior at high doping concentration has been reported for solid PA, PT and emeraldine salt, and even for polyaniline solutions.[3–6] A number of theoretical models have been proposed to explain the evolution of metallic properties in conjugated polymers as a function of dopant concentration. These are based on regular or disordered distribution of charged defects (solitons, polarons, and bipolarons)[7–15] on a single chain. In the present work we present a theoretical study of the oxidation process of PT. The effects on the electronic structure produced by several distributions of defects were analyzed. The following conclusions resulted from our calculations. (i) A regular bipolaron distribution does not produce a metallic state, since a gap in the electronic structure remains at any dopant concentration; (ii) the formation of bipolaron clusters leads to the appearance of extended levels at the Fermi energy at 8 mol % doping level; (iii) doped clusters mixed with disordered bipolaron distributions lead to the metallic state for doping levels in the range 20–30 mol %. We found that the coexistence of large doped and undoped regions in the chain is the most important feature of these defect distributions in order to obtain the metalliclike electronic structure. This is particularly interesting since the metallic state in conjugated polymers has been experimentally characterized by the persistence of specific infrared activity attributed to isolated conformational defects.

In Sec. II we present the methodology we have used, in Sec. III we present and discuss the obtained results.

II. METHODOLOGY

The densities of states (DOS) of long, finite, ordered, and disordered chains are obtained using the negative factor counting (NFC) technique[16] coupled to a tight-binding Hamiltonian. The Hamiltonian matrix elements are obtained from transferred parameters optimized in oligomer calculations using a modified Hückel approach with σ compressibility, as discussed below. The NFC technique allows a fast DOS calculation avoiding the direct diagonalization of the Hamiltonian matrix. The eigenvectors associated with the Fermi energy region are analyzed through the expansion coefficients $\{c_i\}$ of the molecular orbitals from the usual linear combination of atomic orbitals in the p_z base. The coefficients are obtained using the inverse iteration method.[17]

The Hückel method with σ compressibility has been used in different ways for the study of elementary excitations in conducting polymers.[18]

The Hamiltonian is defined as

$$\mathbf{H}=\sum_i |i\rangle\alpha_i\langle i| + \sum_i \{|i\rangle\beta_{i,i+1}\langle i+1| + \text{H.c.}\} + \sum_i f_{i,i+1} \ . \quad (1)$$

In this model the σ electrons are treated in an adiabatic approximation and the π electrons are described in terms of the Hückel theory. The p_z atomic orbitals ($2p_z$ and $3p_z$ for C and S, respectively, in the present case) define the base $\{|i\rangle\}$. The α_i's are the ionization potential values (0.0 and -4.0 eV for C and S, respectively). The resonance integrals $\beta_{i,i+1}$ are calculated using the Coulson relation,

$$\beta_{i,i+1}=A\exp(-R_{i,i+1}/B) \ , \quad (2)$$

where $R_{i,i+1}$ is the distance between neighboring atoms and A and B are adjustable parameters. Starting from a tentative geometry, the system is free to relax in order to minimize the total energy, where $f_{i,i+1}$ represents the σ contribution to the elastic energy and is defined by

$$f_{i,i+1}=C\beta_{i,i+1}(R_{i,i+1}-R_0+B) \ . \quad (3)$$

In Eq. (3), R_0 is the reference bond length and C is a fitting parameter. The parameters A, B, and C are chosen in order to reproduce experimental values measured for the gap, valence bandwidth, and ground-state geometry.

In the present calculations we treated the problem in two steps. First, we have used chains with 20 rings, which are long enough to reproduce the results of the infinite (in the Bloch limit) polymer chain. Geometry optimizations were performed in order to find appropriate parameters for the neutral chain and the doubly charged chain, representing a positive bipolaron. In a second step, a polymer electronic-structure simulation has been carried out for much longer chains.

For the neutral chain, using $R_0=1.557$ and 1.782 Å, respectively, for C-C and C-S, and $A=123.6$ eV, $B=0.3776$ Å and $C=7.814$ Å^{-1}, we have obtained a final geometry in good agreement with experimental data and other theoretical calculations[19–22] (see Table I).

The obtained valence bandwidth was 2.8 eV as compared to 2.5 eV from the *ab initio* quality valence effective Hamiltonian (VEH) calculations.[21] The "gap" value (highest occupied molecular orbital (HOMO)–lowest unoccupied molecular orbital (LUMO) energy difference) also compares well with the experimental value of 2.1 eV from *in situ* optical absorption of electrochemically polymerized samples.[23] The HOMO analysis shows, as expected, that the sulfur atoms contribute very little. These combined results suggest that we have a reliable set of parameters that could be transferred to larger chains.

For the chain with a positive bipolaron defect, two intragap states appear, with associated transition at 1.43 and 2.01 eV and a new gap of 0.62 eV. These results agree well with the respective experimental values of 1.40–1.45, 2.10, and 0.60–0.65 eV, taken from ClO_4-doped polythiophenes.[23] The energy associated with the defect creation is 0.57 eV. This compares with 0.67 eV obtained by Bertho and Jouanin,[24] and 0.66 eV by Brédas, Wudl, and Heeger,[25] calculated by a similar model. The smaller value we have obtained could be explained by the fact that we have not used constraints for defect relaxation in our calculations, as in the other works.

The C-C bondlength alternation pattern, defined as $\Delta r=(-1)^{i+1}(R_{i+1}-R_i)$ [see Fig. 1(b)] shows the expected localization and the characteristic quinoid pattern at the center of the chain. The comparison between the charge distribution of the neutral chain and the one containing a bipolaron does not indicate any significant contributions from the end rings, showing, as expected for this chain size, no important finite-size effects. The geometrical distortions induced by the bipolaron defect are spread over four rings, which contain more than 70%

TABLE I. Geometrical parameters for PT. $R_{C\text{-}S}$, $R_{C\alpha\text{-}C\beta}$, and $R_{C\beta\text{-}C\beta}$ stand for carbon-sulfur, α-carbon–β-carbon, and α-carbon–α-carbon bondlengths, respectively.

Method	$R_{C\text{-}S}$ (Å)	$R_{C\alpha\text{-}C\beta}$ (Å)	$R_{C\beta\text{-}C\beta}$ (Å)	$R_{C\alpha\text{-}C\alpha}$ (Å)
Expt. (Ref. 19)[a]	1.714	1.370	1.423	
Expt. (Ref. 20)[b]	1.717	1.357	1.433	1.480
STO-3G (Ref. 21)[c]	1.721	1.346	1.444	1.480
3-21G (Ref. 22)[c]	1.811	1.341	1.444	1.441
This work[d]	1.721	1.350	1.441	1.457

[a]Microwave data on thiophene.
[b]Gas phase electron diffraction on bithiophene.
[c] *Ab initio* calculations.
[d]20-ring oligomer.

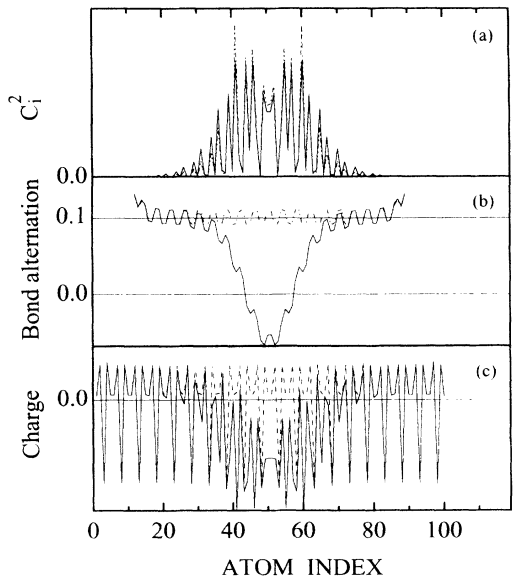

FIG. 1. (a) Wave-function expansion $\{c_i^2\}$ for the first bipolaron level: (——) exact Hückel calculation and (— — —) NFC simulation; (b) C—C bond alternation pattern, and (c) charge distribution associated with (— — —) neutral and (——) doubly charged oligomers. In (b) only C atoms are shown. This figure has been shifted to match the bipolaron distortion on Figs. 1(a) and 1(c).

of the positive charge. Beyond that, the system recovers the neutral chain pattern [Fig. 1(c)]. Based on these results we have chosen one ring (representative of neutral PT) and four rings (representative of a bipolaron) to be the structural units used in the NFC simulation of the electronic structure of neutral and bipolaronic chains, respectively, transferring the Hamiltonian elements from the Hückel calculations. We have also included the appropriate parameters for the edge cells.

Following this procedure, we have obtained, for the NFC simulation of the 20-ring oligomer with a bipolaron distortion, the values of 0.67, 1.55, and 2.19 eV, respectively, for the gap and bipolaronic transitions, in comparison with 0.62, 1.43, and 2.01 eV from the exact Hückel calculation. In Fig. 1(a) we compare the coefficient distribution obtained with the two methods for the first bipolaron level. These results show that four rings are enough to simulate the bipolaron defect, reproducing its main electronic features.

We can build very long chains using these transferred parameters for the NFC simulation and easily control their relative doping concentrations, as well as their spatial distribution. Chains containing up to 100 rings (500 heavy atoms) were used and a direct relationship between the number of dopant species and bipolaron defects has been assumed (2:1). In this work we have investigated the electronic structure of long, finite chains containing ordered and disordered distribution of bipolarons defects as a function of dopant concentration.

III. RESULTS AND DISCUSSIONS

NFC results for a neutral chain with 98 rings show a gap of 2.0 eV and a total π bandwidth of 12.9 eV. As the concentration of bipolarons (orderly and disorderly distributed) increases, the HOMO energy position is redshifted, as well as the Fermi energy, in accordance with some experimental data.[26] This shows that the transfer of parameters from Hückel oligomers is reproducing well the main electronic features of very long chains.

In Fig. 2 we show the gap evolution as a function of the defect concentration (orderly distributed). As we can see from the figure, the gap persists even in the case of maximum doping (only quinoid rings are present), with a limiting value of 0.23 eV. In a slightly disordered defect distribution, introduced by a small variation in the number of neutral rings between bipolarons [see Fig. 2], the gap value is further reduced, although this reduction is not sufficient that we could associate it with the semiconductor-to-metal transition. These results show that an ordered or slightly disordered distribution of defects cannot describe the metallic regime observed in polythiophenes. This is also true for polyacetylene and polyanilines, as has been shown by other authors using different approaches.[13,15]

Considering that some disorder is always present even in the best PT samples produced today, it is reasonable to assume a nonuniform doping, with heavily doped regions in contrast to lightly doped ones. In order to simulate this situation, we built chains where we allowed the formation of bipolaron clusters. In Fig. 3 we show the gap and DOS evolution as a function of defect concentration for a chain containing 98 rings with a central bipolaron cluster. The results are not very sensitive to the relative position of the cluster inside the chain. We note that for $y = 10$ mol %, i.e., a cluster of five bipolarons, we have already a very small HOMO-LUMO energy separation and a finite DOS at the Fermi energy. The gap value quickly saturates and remains constant until y (dopant content) approaches the value corresponding to a bipolaron lattice. This is an unexpected result if we consider that for $y = 48$ mol %, a gap of 0.23 eV is still present in an ordered distribution of defects.

The analysis of the eigenvectors associated with the eigenvalues in the Fermi region shows that they are delocalized over the whole chain. In Fig. 4 are depicted the $\{c_i^2\}$ associated with the HOMO for the cases $y = 16$ and 26 mol %, respectively, where the bipolaron cluster is located at the central part of the chain. The probability densities show different amplitudes for the aromatic and quinoid regions, as expected from the energy differences associated with the two different configurations. It is to be noted that the amplitudes at the quinoid region in-

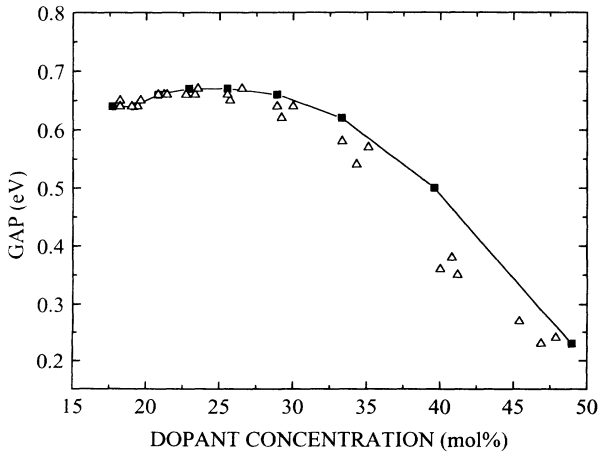

FIG. 2. Gap vs dopant concentration for (■) ordered and (△) lightly disordered bipolaron distributions.

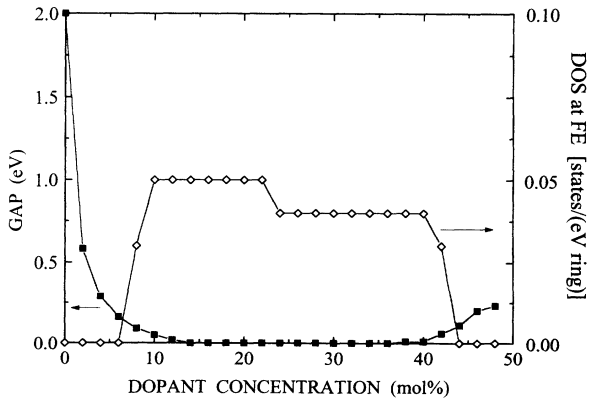

FIG. 3. Gap energy (■) and density of states at Fermi energy (◇) as a function of dopant concentration for a bipolaron cluster. The arrows indicate the appropriate axis for each curve.

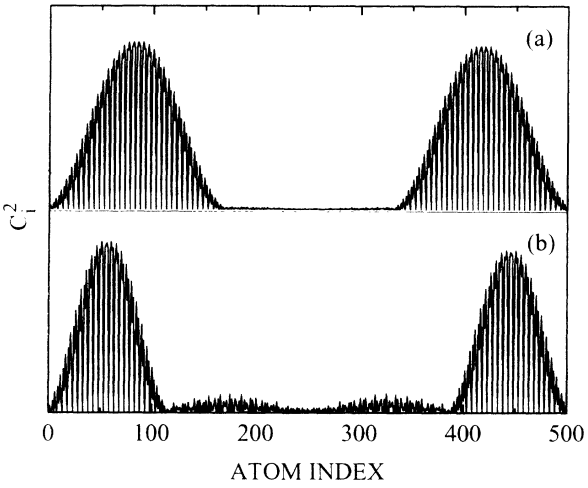

FIG. 4. Wave-function expansion coefficients $\{c_i^2\}$ of HOMO state for the cases (a) 16 mol % and (b) 26 mol %.

crease as the bipolaron cluster increases and that the amplitudes are finite everywhere in the chain. This kind of quantum state is not periodic as the one obtained for a regular distribution of defects but allows the electron to move from one region of large probability to another; that is, the scattering at the quinoid region has a large transmission probability. In Fig. 5 the densities of states are plotted as a function of y (ranging from 0–24 %) for chains containing 100 rings. It can be seen from the figure that as y increases, new states are created in the original gap region, leading to gap closure. These results together clearly indicate that the bipolaron clustering induces a metallic transition as we have a combined gapless HOMO-LUMO structure, and a finite DOS at the Fermi energy with the presence of extended states.

However, we cannot expect the formation of large bipolaron clusters more or less orderly distributed, since this would require an unusual coupling between dopants along the chains. A more realistic expectation is a disordered distribution of bipolarons, including clustering formation.

In order to verify whether a disordered distribution of bipolarons could lead to the metallic behavior observed above, we carried out calculations over many configurations using a weighted random-number generator in order to better control the y concentration.

Our results show that a generic disordered distribution of bipolaron leads to the disappearance of the gap only when a bipolaron cluster and a large region of aromatic rings coexist. In a random distribution, the chance of the appearance of this type of configuration is not a direct function of y, but a probabilistic feature. However, as we expect, the onset of the metallic regime is a direct function of y. The analysis of the eigenfunctions at the Fermi energy shows that there is a minimum size limit for the clusters in order to induce the transition to the metallic regime. With the set of present parameters, the required number of bipolarons is 7 (in comparison with 4, for the case where a single cluster is assumed), which implies a minimum concentration of $y = 14$ mol %. In addition, the existence of aromatic regions containing at least six rings is also required. Once these conditions are satisfied, the metallic transition is observed (Fig. 6).

These results strongly suggest that disorder can be an important mechanism of inducing a metallic transition when it includes some amount of segregation, i.e., when it favors the existence of bipolaron clusters separated by aromatic regions. One explanation for this behavior could be drawn by symmetry arguments. It is well known that HOMO and LUMO wave functions of PT belong to the same irreducible representation of the symmetry point group. Based on this, it has been argued that no intermediate structure for PT, between the purely aromatic and the purely quinoid ones, could exist to obtain a gapless chain, since the HOMO and LUMO bands interact and avoid crossing.[27] Another aspect of the wave

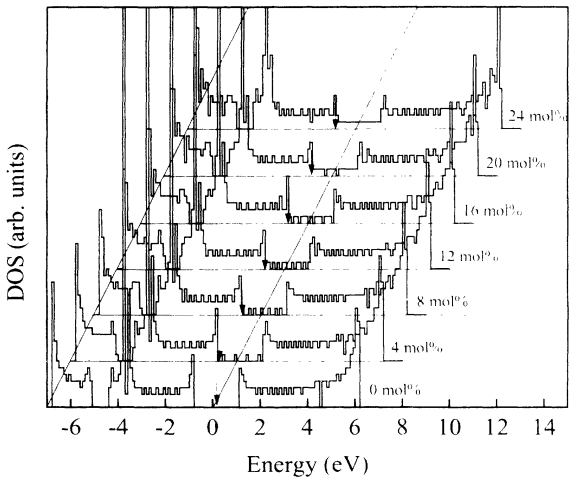

FIG. 5. Density of states histograms for bipolaron clusters with y ranging from 0.0–24.0 mol %. Arrows indicate the position of the Fermi energy.

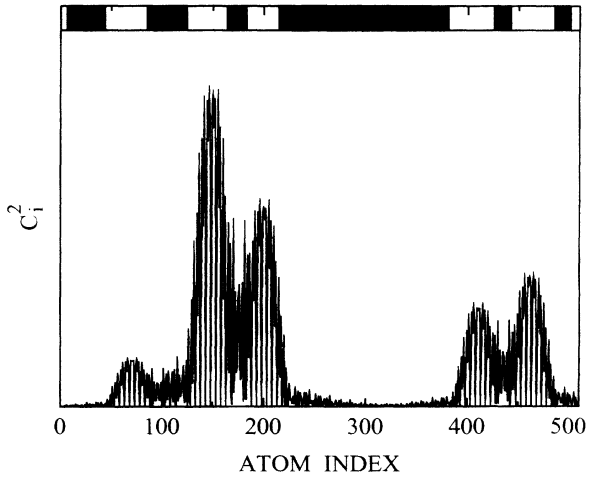

FIG. 6. HOMO wave-function expansion coefficients $\{c_i^2\}$ for the bipolaron distribution sketched on the top, where filled regions correspond to bipolarons. The large cluster in the middle of the chain contains eight bipolarons.

function's symmetry is that, for an aromatic chain, the HOMO state makes a very small contribution on sulfur atoms and the bonding character between α and β carbons inside one ring, while the LUMO state makes a significant contribution on sulfur and the bonding character between both β carbons. In the quinoid chain structure, these features are interchanged, i.e., the HOMO wave function has a similar symmetry of the corresponding LUMO state in the aromatic structure. When a bipolaron cluster is allowed to form in an otherwise aromatic PT chain, the resulting electronic wave functions have mixed character and symmetry is lost—for instance, there is a much more important contribution of sulfur atoms on the HOMO wave function, even in the aromatic region. In terms of the corresponding one-electron energies in the band edges, this mixing tends to destabilize the state at the aromatic region and stabilize the state at the quinoid region, with the opposite situation occurring for the lowest unoccupied states. As a consequence, the HOMO-LUMO separation vanishes at some point. However, both regions—aromatic and quinoid—have to be large enough in order that the symmetry breaking does not appear as a local feature. This explains the trends observed in Fig. 3, for which a band gap exists for lightly and heavily doped PT; in the first case, aromatic regions are much larger than the quinoid ones, and the opposite situation occurs in the second case. A similar situation is expected to be found in polymers having the same symmetry properties, as poly-*p*-phenylene and polypyrrole, but not in *trans*-polyacetylene, which has a degenerate ground state.

These conclusions seem to be in agreement with experimental results obtained by small-angle neutron scattering on the structure of doped PT in solution,[28] which are consistent with a nonhomogeneous doping of the chains and, possibly, with dopant condensation.

On the basis of the present results, one could speculate that the combined use of different dopants (different diffusion coefficients) on the same sample might reduce the critical dopant concentration (y_{crit}) needed to achieve the metallic states as compared to the effect produced by each dopant alone.

ACKNOWLEDGMENTS

The authors acknowledge financial support from Conselho Nacional de Desenvolvimento Científico e Tecnológico (CNPq), Coordenadoria de Aperfeiçoamento de Pessoal de Ensino Superior (CAPES) and Fundação de Amparo à Pesquisa do Estado de São Paulo (FAPESP). One of us (D.S.G.) thanks Professor Z. G. Soos for valuable discussions and his kind hospitality in Princeton.

*Permanent address: Departamento de Física, UNESP-Bauru, 17033 Bauru, São Paulo, Brazil.

[1]For a review on recent progress see, for instance, *Proceedings of the International Conference on Science and Technology of Synthetic Metals, 1992* [Synth. Metals (to be published)].

[2]A. J. Heeger, S. Kivelson, J. R. Schrieffer, and W. P. Su, Rev. Mod. Phys. **60**, 781 (1988).

[3]S. Ikehata, J. Kaufer, T. Woener, A. Pron, M. A. Druy, A. Sivak, A. J. Heeger, and A. G. MacDiarmid, Phys. Rev. Lett. **45**, 1123 (1980).

[4]K. Mizoguchi, K. Misuo, K. Kume, K. Kaneto, T. Shiraishi, and K. Yoshino, Synth. Metals **18**, 195 (1987); F. Moraes, D. Davidov, M. Kobayashi, T. C. Chung, J. Chen, A. J. Heeger, and F. Wudl, *ibid.* **10**, 169 (1985).

[5]J. M. Ginder, A. F. Richter, A. G. MacDiarmid, and A. J. Epstein, Solid State Commun. **63**, 97 (1987).

[6]Y. Cao and A. J. Heeger, Synth. Metals **52**, 193 (1992).

[7]E. J. Mele and M. J. Rice, Phys. Rev. B **23**, 5397 (1981).

[8]A. J. Epstein, in *Handbook of Conducting Polymers,* edited by A. Skotheim (Dekker, New York, 1986), Ref. 1, p. 1041.

[9]S. Kivelson and A. J. Heeger, Phys. Rev. Lett. **55**, 308 (1985).

[10]H. Y. Choi and E. J. Mele, Phys. Rev. B **34**, 8750 (1986).

[11]S. Stafström, J. L. Brédas, A. J. Epstein, H. S. Woo, D. B. Tanner, W. S. Huang, and A. G. MacDiarmid, Phys. Rev. Lett. **59**, 1464 (1987).

[12]E. N. Conwell and S. Jeyadev, Phys. Rev. Lett. **61**, 361 (1988).

[13]D. S. Galvão, D. A. dos Santos, B. Laks, C. P. de Melo, and M. J. Caldas, Phys. Rev. Lett. **63**, 786 (1989).

[14]D. H. Dunlap, H. L. Wu, and P. W. Phillips, Phys. Rev. Lett. **65**, 88 (1990).

[15]F. C. Lavarda, D. S. Galvão, and B. Laks, Phys. Rev. B **45**, 3107 (1992).

[16]P. Dean, Proc. R. Soc. London A **254**, 507 (1960).

[17]J. H. Wilkinson, *The Algebraic Eigenvalue Problem* (Clarendon, Oxford, 1965), p. 633.

[18]J. L. Brédas, R. R. Chance, and R. Silbey, Phys. Rev. B **26**, 5643 (1982); M. C. dos Santos and J. L. Brédas, Phys. Rev. Lett. **62**, 2499 (1989).

[19]B. Bak, D. Christhensen, W. B. Dixon, L. Hansen-Nygaard, J. Rastrup-Andersen, and M. Schottländer, J. Mol. Spectrosc. **9**, 124 (1962).

[20]A. Almenningen, O. Bastiansen, and P. Svendsäs, Acta. Chem. Scand. **12**, 1671 (1958).

[21]J. L. Brédas, B. Thémans, J. G. Fripiat, J. M. André, and R. R. Chance, Phys. Rev. B **29**, 6761 (1984).

[22]J. L. Brédas and A. J. Heeger, Macromolecules **23**, 1150 (1990).

[23]T.-C. Chung, J. H. Kaufman, A. J. Heeger, and F. Wudl, Phys. Rev. B **30**, 702 (1984).

[24]D. Bertho and C. Jouanin, Phys. Rev. B **35**, 626 (1987).

[25]J. L. Brédas, F. Wudl, and A. J. Heeger, Solid State Commun. **63**, 577 (1987).

[26]M. Logdlund, R. Lazzaroni, S. Stafström, W. R. Salaneck, and J. L. Brédas, Phys. Rev. Lett. **63**, 1841 (1989).

[27]J. L. Brédas, J. Chem. Phys. **82**, 3808 (1985).

[28]J. P. Aimé, in *Conjugated Polymers: The Novel Science and Technology of Highly Conducting and Nonlinear Optically Active Materials,* edited by J. L. Brédas and R. Silbey (Kluwer, Dordrecht, 1991), p. 229.